NANO LETTERS

2009
Vol. 9, No. 9
3318-3322

Electrolyte-Gated Graphene Field-Effect Transistors for Detecting pH and Protein Adsorption

Yasuhide Ohno,* Kenzo Maehashi, Yusuke Yamashiro, and Kazuhiko Matsumoto

The Institute of the Scientific and Industrial Research, Osaka University, 8-1 Mihogaoka, Ibaraki, Osaka 567-0047, Japan

Received May 20, 2009; Revised Manuscript Received July 13, 2009

ABSTRACT

We investigated electrolyte-gated graphene field-effect transistors (GFETs) for electrical detecting pH and protein adsorptions. Nonfunctionalized single-layer graphene was used as a channel. GFETs immersed in an electrolyte showed transconductances 30 times higher than those in a vacuum and their conductances exhibited a direct linear increase with electrolyte pH, indicating their potential for use in pH sensor applications. We also attempted to direct surface-protein adsorption and showed that the conductance of GFETs increased with exposure to a protein at several hundred picomolar. The GFETs thus acted as highly sensitive electrical sensors for detecting pH and biomolecule concentrations.

Electrical detection of chemical and biological species using novel nanomaterial devices, such as silicon nanowires and carbon nanotubes, has attracted significant attention[1−10] for genomics, clinical diagnosis, and practical pharmacy applications during the past decade, because conventional optical detection methods require highly advanced knowledge of techniques and complex labeling processes. Electrical detection methods exhibit highly sensitive detection of chemical and biological species because the surface−analyte or analyte−analyte bindings occur very close to the channel. Although carbon nanotube field-effect transistors (CNT-FETs) are one of the most promising candidates for label-free biosensors[4−10] because of their small diameters and high aspect ratios, the absolute values of their drain current depend on their diameters and the work function of the electrode metal.[11] This variation in the device characteristics is an obstacle to device reliability, and the control of the diameter of carbon nanotubes (i.e., the chirality of carbon nanotubes) is a major problem.[12] Recently, to resolve these problems aligned carbon nanotubes, synthesized on quartz substrates and their logic circuits have been reported.[13−15] In addition, conventional CNT-FETs have been shown to exhibit p-type characteristics in air and electrolytes,[4,7−10] but they can detect only positively charged species in electrolytes due to their band structure.[16]

Graphene is a single layer of the graphite that has the potentials to resolve the problems with CNT-FETs. They are ideal two-dimensional crystals that show an extremely high mobility of $\sim 10^4$ cm^2 V^{-1} s^{-1} and large carrier capacities of $\sim 10^{12}$ cm^{-2} even at room temperature without doping.[17−23] Because their electrical characteristics are sensitively influenced by surface conditions, gas molecule sensors using graphene field-effect transistors (GFETs) have been reported.[19] Although many electrical characteristics of GFETs have been described, investigations into the electrical detection of chemical and biological species using GFETs have been only just begun.[24−26] The mechanism of action for GFET sensors is that chemical or biological species adsorbed on the surface of the graphene act as electron donors or acceptors, resulting in conductance changes. To realize GFET biological sensors, it is important to investigate the electrical characteristics under low-electrical field due to avoidance of biomolecule oxidization. In this paper, we describe our attempts to apply GFETs to chemical and biological sensors. We investigated behavior of GFETs immersed in an electrolyte and show that they have very good transfer characteristics compared with their characteristics in vacuum. They also exhibit clear pH-dependent conductance characteristics and could electrically detect surface-protein adsorption. Thus, we demonstrate the achievement of electrical detection of biomolecules with GFETs.

The graphene single-layer crystals were obtained from natural graphite by mechanical exfoliation. The device was fabricated on a 285 nm thick SiO_2 layer, thermally grown on a degenerately doped silicon substrate ($\rho < 0.01$ Ω cm). In this work, a single-layer graphene was used for the FETs' channel, confirmed by Raman spectroscopy (see Supporting

* To whom correspondence should be addressed. E-mail: ohno@sanken.osaka-u.ac.jp.

10.1021/nl901596m CCC: $40.75
Published on Web 07/28/2009

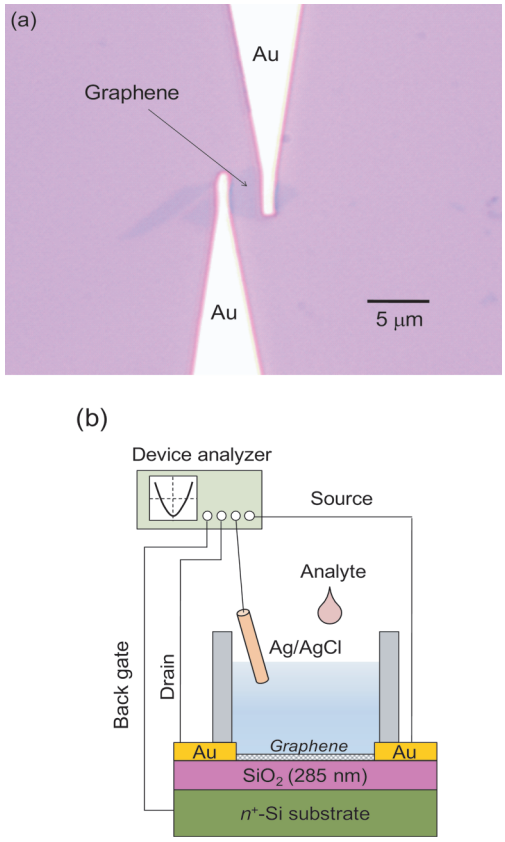

Figure 1. (a) Optical micrograph of a typical GFET. (b) Schematic illustration of the experimental setup for electrolyte-gated GFETs.

Information, Figure S1 and Figure S2). Figure 1a shows an optical micrograph of a typical GFET. The typical size of graphene obtained by this method was 10 μm. Ti/Au (5 nm/30 nm) source and drain electrodes were formed by conventional e-beam lithography, metal deposition, and a lift-off method. The degenerately doped silicon substrate was also used for the back gate. Various pH solutions were made by mixing a 10 mM phthalate buffer solution at pH 4.0, a 10 mM phosphate buffer solution at pH 6.8, and a 10 mM borate buffer solution at pH 9.3. The leakage current between the solution and the Au electrodes was found to be negligible (less than 10 nA; see Supporting Information, Figure S3).

Initially, we investigated the transport behaviors of GFETs in electrolytes. In an electrolyte, the electrical-double layer acts as a top-gate insulator with a thickness defined generally by the Debye−Hückel equation, that is, the thickness depends on the ionic strength and is as small as 1−5 nm in an electrolyte with a concentration of several millimolars. This is very thin, compared with recently reported top-gate GFETs with 15 nm thick HfO_2.[21] Electrolyte-gated CNT-FETs and GFETs have shown good electrical characteristics as thin top-gate insulators with high dielectric constants in ionic solutions.[25,27−29] Figure 1b shows the experimental measurement system. The GFETs were immersed in the electrolyte and a silicone rubber well was placed on the GFETs to allow the surface of the graphene channel to be filled with several buffer solutions and analytes for electrical measurement and sensing. An Ag/AgCl reference electrode (BAS Inc., Tokyo, Japan) was used as the top-gate electrode to minimize environmental effects.[30] The electrical characteristics of the GFETs were measured by a semiconductor parameter analyzer (4156C; Agilent technologies Inc., Santa Clara, CA), using two-terminal measurement.

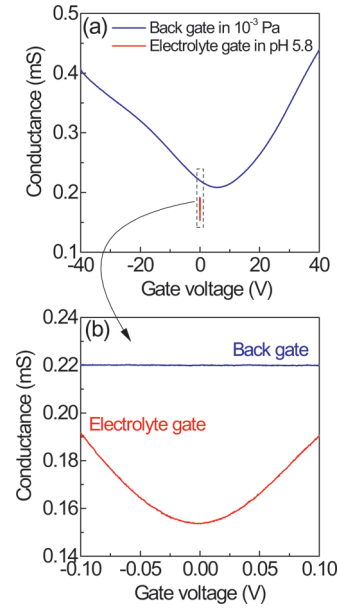

Figure 2. (a) Conductance as a function of back-gate voltage at 10^{-3} Pa and top-gate voltage in an electrolyte at pH 5.8. (b) Enlarged view of conductance as a function of gate voltage.

Figure 2 shows conductance (G) plotted against the back-gate voltage (V_{BGS}) and top-gate voltage (V_{TGS}) of a typical GFET in 10^{-3} Pa and in an electrolyte (pH 5.8) at room temperature. Figure 2b shows the enlarged view of the Figure 2a. Ambipolar electric field-effect characteristics of a GFET were observed for both back-gate and top-gate operation. Transconductance (g_m) of the GFET was estimated to be 1.0 and 36 μS in a vacuum and the electrolyte, respectively, at 295 K, indicating the formation of a very thin top-gate insulator in the electrolyte. To clarify the difference between the g_m values of the devices, back- and top-gate capacitances were estimated using a simple model. Assuming that graphene is equivalent to a metal disk placed on the insulator, the gate capacitance can be expressed by the equation below[31]

$$C_G = \frac{2\pi\varepsilon_0(\varepsilon_r + 1)r}{\tan^{-1}\left[\frac{2h(\varepsilon_r + 1)}{r\varepsilon_r}\right]}$$

where, r, h, ε_r, and ε_0 are the radius of the metal disk (graphene), the thickness of the gate insulator, the relative permittivity, and vacuum permittivity, respectively. For the electrolyte-gated GFETs (with $r = 1.5$ μm, $h = 1$ nm, and ε_r (H_2O) = 80), the estimated electrostatic gate capacitance was $C_{G\_EL} \sim 500$ nF cm^{-2}. In this case, if total top-gate capacitance (C_{TG}) is considered as a series of the C_{G_EL} and the quantum capacitance (C_Q),[21,28] then $C_{TG} = C_{G\_EL}C_Q/(C_{G\_EL} + C_Q)$. Because the C_Q of the graphene channel is approximately 2 μF cm^{-2},[21] the C_{TG} is 400 nF cm^{-2}. This

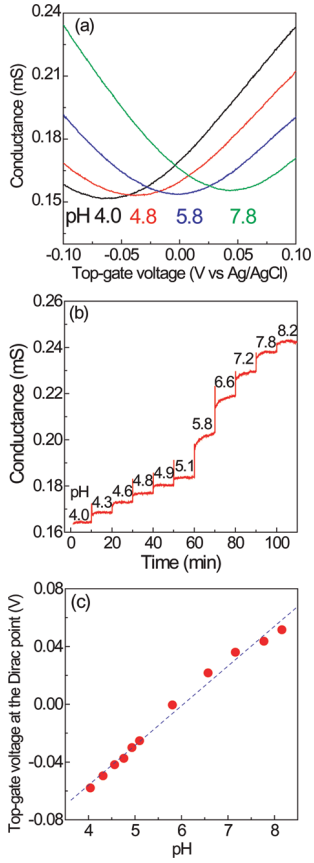

Figure 3. (a) Conductance as a function of top-gate voltage of a GFET at pH 4.0, 4.8, 5.8, and 7.8. (b) Conductance versus time data of a GFET for pH values from 4.0 to 8.2. (c) Top-gate voltage at the Dirac point as a function of pH. The dashed line is a linear fit to the data points.

value is more than 3 orders of magnitude larger than the back-gate capacitance of 85 pF cm^{-2} (with $r = 1.5\ \mu$m, $h =$ 285 nm, and ε_r (SiO_2) = 3.9), given by the above equation. It can be concluded that this larger top-gated capacitance gave rise to better transfer characteristics of GFETs in the electrolyte, indicating their high potentials for use in field-effect sensing applications.

The dependence of the transfer characteristics and conductance of GFETs on pH were evaluated. Figure 3a shows conductance plotted as a function of V_{TGS} for a GFET in various electrolytes at various pH values from 4.0 to 7.8. The Dirac points of the GFET shifted in a positive direction with increasing pH. This behavior indicates that GFETs can detect the pH value by the electrical characteristics. A plot of the time-dependent conductance for a GFET at $V_{TGS} =$ −80 mV in pH values from 4.0 to 8.2. is shown in Figure 3b. Every 10 min, either a 10 mM phosphate buffer solution at pH 6.8 or a 10 mM borate buffer solution at pH 9.3 was added to increase the pH. The conductance increased stepwise with pH from 4.0 to 8.2, and the conductance at each pH value was virtually constant. The plot of the Dirac point voltages against pH values indicates that the relationship between pH and conductance is linear over the range from 4.0 to 8.2, as shown in Figure 3c. Similar changes in gate transfer characteristics have been observed for a GFET exposed to NO_2.[19] It is concluded that the increased conductance can be attributed to the increased negative charge around the graphene channel, because the hole is the carrier in this condition. Increased conductance has also been observed in carbon nanotube pH sensors, which has been interpreted as the attachment of hydroxide ions, that act as electron scavengers.[32,33] We believe these phenomena can occur on the graphene channel and the results indicate that GFETs can be used as pH sensors.

It should be noted that the Dirac point of GFETs at a pH solution was not constant. Although the Dirac point = 0 V was realized at pH 5.8 in this device, other devices showed the Dirac point = 0 V at different pH values. One possible reason of the instability is due to charged impurities such as residual EB resist, defects or underlying SiO_2 and Si. Indeed, the solution pH slightly influenced the carrier mobility (see Supporting Information, Figure S4). Charged impurity scattering is major subject in the graphene technology.[34,35] These uncontrollable charged impurities may lead the Dirac point instability.

Finally, we demonstrated label-free biomolecule detection, based on electrolyte-gated GFETs. A 10 mM phosphate buffer electrolyte solution at pH 6.8 was used with a bovine serum albumin (BSA; Sigma Aldrich Inc., St Louis, MO) target biomolecule. The isoelectric point of BSA is 5.3, indicating that BSA molecules are negatively charged at the pH used for this measurement. Figure 4a shows the evolution of conductance of a GFET for electronic monitoring of BSA adsorption on a graphene channel at $V_{TGS} = -0.1$ V and $V_{BGS} = 0$ V. Under this condition, the conductance was expected to be increased by the hole carrier when (negatively charged) BSA was attached to the graphene. Measurement began with a 10 mM pure phosphate buffer solution. After 10 min, further pure buffer solution was added and the conductance was virtually unchanged. After 20 min, BSA concentration dependence of the conductance was shown. Arrows in Figure 4a mark the points where solutions were changed. The conductance clearly increased when BSA was introduced, indicating adsorption on the graphene surface. The conductance change (ΔG) is shown as a function of BSA concentration (C_{BSA}) in Figure 4b. ΔG increased linearly at low concentrations and was saturated at higher concentrations. This result indicates that the adsorption of BSA molecules onto the graphene surface follows the Langmuir adsorption isotherm given by

$$\frac{C_{BSA}}{\Delta G} = \frac{C_{BSA}}{\Delta G_{Max}} + \frac{K_d}{\Delta G_{Max}}$$

where K_d is the dissociation constant of the interaction between BSA molecules and graphene and ΔG_{Max} is the conductance at saturation. The Langmuir adsorption isotherm fitted the experimental results well, as shown in Figure 4c. The K_d was estimated to be 1.5×10^{-8} M, which was comparable with the values obtained for Si nanowire[1] and CNT-FET[8,9] biosensors using antibody−antigen interactions, despite the fact that BSA molecules were considered to be directly adsorbed onto the graphene surface in this work

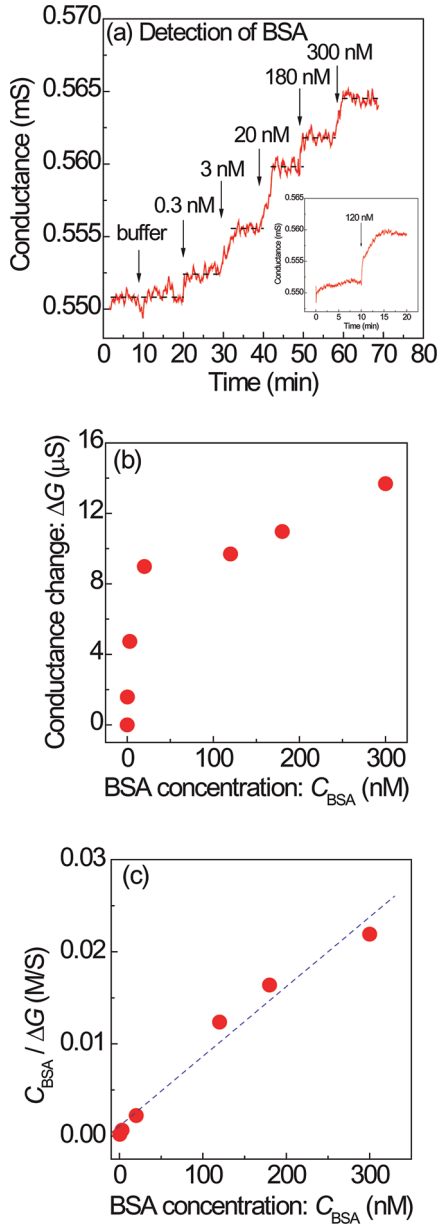

Figure 4. (a) Conductance versus time for electrical monitoring of exposure to various BSA concentrations. Dashed lines indicate the average conductance. The inset shows the time dependence of the conductance at adding the 120 nM BSA. (b) Plot of the conductance change of a GFET versus BSA concentration. (c) BSA concentration per conductance change ($C_{BSA}/\Delta G$) as a function of BSA concentration. The dashed line is a linear fit to the Langmuir adsorption isotherm.

rather than through a protein−protein interaction. Further experiments are needed to confirm the suitability of the Langmuir adsorption isotherm for these experimental results.

In this work, the conductance changes by BSA adsorption were quite small. Three possible interpretations can be considered for the small conductance changes. One interpretation is due to the electrode-graphene contact resistance. Although two-terminal measurement was used in this experiment, four-terminal measurement is needed to ignore the contact resistance fluctuations. Another interpretation is due to desorption of the BSA molecules. Protein sensing using specific protein detection such as antigen−antibody effect can efficiently interrupt the BSA desorption. The other interpretation is due to the difference between isoelectric point of the BSA (=5.6) and solution pH (=6.8) is relatively small. This small difference may lead some uncharged amino acid of the BSA molecules. Moreover, it is important to clarify where the charge transfer occurs and surface area dependence of the protein adsorption. These subjects should be investigated to develop the biomolecule detector using GFETs.

In conclusion, we investigated electrolyte-gated GFETs for chemical and biological detectors. The GFETs showed good gate transfer characteristics in electrolytes; their transconductances were 30 times larger than those obtained under vacuum. Clear pH-dependent conductance was observed, indicating the potential for use of GFETs in pH sensors. Moreover, their conductance showed protein-concentration dependence and their conductance changes with BSA concentration were fitted well by the Langmuir adsorption isotherm. These results indicate that GFETs are promising candidates for the development of real-time chemical and biological sensors.

Acknowledgment. This research was partially supported by Core Research for Evolutional Science and Technology (CREST), the Japan Science and Technology Corporation (JST), and a Grant-in-Aid for Scientific Research from the Japan Society for the Promotion of Science (No. 19054011). The authors were also supported in part by a Grant-in-Aid for Scientific Research and Special Education and Research Expenses (Post-Silicon Materials and Devices Research Alliance) from the Japan Society for the Promotion of Science. Natural graphite used in this work was kindly provided by Nippon Graphite Industries Ltd.

Supporting Information Available: Details of confirmation of single-layer graphene used in this work, ionic conductivity, pH dependence of the carrier mobility, and hole doping by BSA adsorption were described. This material is available free of charge via the Internet at http://pubs.acs.org.

References

(1) Cui, Y.; Wei, Q.; Park, H.; Lieber, C. M. *Science* **2001**, *293*, 1289.
(2) Zheng, G.; Patolsky, F.; Cui, Y.; Wang, U. W.; Lieber, C. M. *Nat. Biotechnol.* **2005**, *23*, 1294.
(3) Elfström, N.; Karlström, A. E.; Linnros, J. *Nano Lett.* **2008**, *8*, 945.
(4) Chen, R. J.; Bangsaruntip, S.; Drouvalakis, K. A.; Kam, N. W. S.; Shim, M.; Li, Y.; Kim, W.; Utz, P. J.; Dai, H. *Proc. Natl. Acad. Sci. U.S.A.* **2003**, *100*, 4984.
(5) Besteman, K.; Lee, J. O.; Wiertz, F. G. M.; Heering, H. A.; Dekker, C. *Nano Lett.* **2003**, *3*, 727.
(6) Lu, Y.; Bangsaruntip, S.; Wang, X.; Zhang, L.; Nishi, Y.; Dai, H. *J. Am. Chem. Soc.* **2006**, *128*, 3518.
(7) Maehshi, K.; Katsura, T.; Kerman, K.; Takamura, Y.; Matsumoto, K.; Tamiya, E. *Anal. Chem.* **2007**, *79*, 782.
(8) Abe, M.; Murata, K.; Ataka, T.; Matsumoto, K. *Nanotechnology* **2008**, *19*, 045505.
(9) Maehashi, K.; Matsumoto, K.; Takamura, Y.; Tamiya, E. *Electroanalysis* **2009**, *21*, 1285.
(10) Martínez, M. T.; Tseng, Y. C.; Ormategui, N.; Loinaz, I.; Eritja, R.; Bokor, J. *Nano Lett.* **2009**, *9*, 530.
(11) Chen, Z.; Appenzeller, J.; Knoch, J.; lin, Y.; Avouris, P. *Nano Lett.* **2005**, *5*, 1497.
(12) Maehashi, K.; Ohno, Y.; Inoue, K.; Maehashi, K. *Appl. Phys. Lett.* **2004**, *85*, 858.

(13) Kang, S. J.; Kocabas, C.; Ozel, T.; Shim, M.; Pimparkar, N.; Alam, M. A.; Rotkin, S. V.; Rogers, J. A. *Nat. Nanotechnol.* **2007**, *2*, 230.
(14) Wang, C.; Ryu, K.; Badmaev, A.; Patil, N.; Lin, A.; Mitra, S.; Wong, H. S. P.; Zhou, C. *Appl. Phys. Lett.* **2008**, *93*, 033101.
(15) Ryu, K.; Badmaev, A.; Wang, C.; Lin, A.; Patil, N.; Gomez, L.; Kumar, A.; Mitra, S.; Wong, H. S. P.; Zhou, C. *Nano Lett.* **2009**, *9*, 189.
(16) Li, C.; Curreli, M.; Lei, B.; Ishikawa, F. N.; Datar, R.; Cote, R. J.; Thompson, M. E.; Zhou, C. *J. Am. Chem. Soc.* **2005**, *127*, 12484.
(17) Novoselov, K. S.; Geim, A. K.; Morozov, S. V.; Jiang, D.; Zhang, Y.; Dubonos, S. V.; Grigorieva, I. V.; Firsov, A. A. *Science* **2004**, *306*, 666.
(18) Novoselov, K. S.; Geim, A. K.; Morozov, S. V.; Jiang, D.; Katsnelson, M. I.; Grigorieva, I. V.; Dubonos, S. V.; Firsov, A. A. *Nature* **2005**, *438*, 197.
(19) Schedin, F.; Geim, A. K.; Morozov, S. V.; Hill, E. W.; Blake, P.; Katsnelson, M. I.; Novoselov, K. S. *Nat. Mater.* **2007**, *6*, 652.
(20) Han, M. Y.; Özyilmaz, B.; Zhang, Y.; Kim, P. *Phys. Rev. Lett.* **2007**, *98*, 206805.
(21) Meric, I.; han, M. Y.; Young, A. F.; Ozyilmaz, B.; Kim, P.; Shepard, K. L. *Nat. Nanotechnol.* **2008**, *3*, 654.
(22) Elias, D. C.; Nair, R. R.; Mohiuddin, T. M. G.; Morozov, S. V.; Blake, P.; Halsall, M. P.; Ferrari, A. C.; Katsnelson, D. W.; Geim, A. K.; Novoselov, K. S. *Science* **2009**, *323*, 610.
(23) Nagashio, K.; Nishimura, T.; Kita, K.; Toriumi, A. *Appl. Phys. Express* **2009**, *2*, 025003.
(24) Mohanty, N.; Berry, V. *Nano Lett.* **2008**, *8*, 4469.
(25) Ang, P. K.; Chen, W.; Wee, A. T. S.; Loh, K. P. *J. Am. Chem. Soc.* **2008**, *130*, 14392.
(26) Sundaram, R. S.; Navarro, C. G.; Balasubramanian, K.; Burghard, M.; Kern, K. *Adv. Mater.* **2008**, *20*, 3050.
(27) Krüger, M.; Buitelaar, M. R.; Nussbaumer, T.; Schönenberger, C.; Forró, L. *Appl. Phys. Lett.* **2001**, *78*, 1291.
(28) Rosenblatt, S.; Yaish, Y.; Park, J.; Gore, J.; Sazonova, V.; McEuen, P. L. *Nano Lett.* **2002**, *2*, 869.
(29) Das, A.; Pisana, S.; Chakraborty, B.; Piscanec, S.; Saha, S. K.; Waghmare, U. V.; Novoselov, K. S.; Krishnamurthy, H. R.; Geim, A. K.; Ferrari, A. C.; Sood, A. K. *Nat. Nanotechnol.* **2008**, *3*, 210.
(30) Minot, E. D.; Janssens, A. M.; Heller, I.; Dekker, H. A. H. C.; Lemay, S. G. *Appl. Phys. Lett.* **2007**, *91*, 093507.
(31) Gelmont, B.; Shur, M. S.; Mattauch, R. J. *Solid-State Electron.* **1995**, *38*, 731.
(32) Pan, H.; Feng, Y. P.; Lin, J. Y. *Phys. Rev. B* **2004**, *70*, 245425.
(33) Lee, K.; Kwon, J. H.; Cho, S. M. W. S.; Ju, B. K.; Lee, Y. H. *Mater. Lett.* **2007**, *61*, 3201.
(34) Chen, J. H.; Jang, C.; Adam, S.; Fuhrer, M. S.; Williams, E. D.; Ishigami, M. *Nat. Phys.* **2008**, *4*, 377.
(35) Chen, F.; Xia, J.; Tao, N. *Nano Lett* **2009**, *9*, 1621.

NL901596M